

Cytoplasmic Lipid Droplets Are Sites of Convergence of Proteasomal and Autophagic Degradation of Apolipoprotein B[□]

Yuki Ohsaki,* Jinglei Cheng,* Akikazu Fujita,* Toshinobu Tokumoto,[†] and Toyoshi Fujimoto*

*Department of Anatomy and Molecular Cell Biology, Nagoya University Graduate School of Medicine, Nagoya 466-8550, Japan; and [†]Department of Biology and Geosciences, Faculty of Science, Shizuoka University, Shizuoka 422-8529, Japan

Submitted July 21, 2005; Revised March 22, 2006; Accepted March 24, 2006
Monitoring Editor: Jeffrey Brodsky

Lipid esters stored in cytoplasmic lipid droplets (CLDs) of hepatocytes are used to synthesize very low-density lipoproteins (VLDLs), into which apolipoprotein B (ApoB) is integrated cotranslationally. In the present study, by using Huh7 cells, derived from human hepatoma and competent for VLDL secretion, we found that ApoB is highly concentrated around CLDs to make “ApoB-crescents.” ApoB-crescents were seen in <10% of Huh7 cells under normal conditions, but the ratio increased to nearly 50% after 12 h of proteasomal inhibition by *N*-acetyl-L-leuciny-L-leuciny-L-norleucinal. Electron microscopy showed ApoB to be localized to a cluster of electron-lucent particles 50–100 nm in diameter adhering to CLDs. ApoB, proteasome subunits, and ubiquitinated proteins were detected in the CLD fraction, and this ApoB was ubiquitinated. Interestingly, proteasome inhibition also caused increases in autophagic vacuoles and ApoB in lysosomes. ApoB-crescents began to decrease after 12–24 h of proteasomal inhibition, but the decrease was blocked by an autophagy inhibitor, 3-methyladenine. Inhibition of autophagy alone caused an increase in ApoB-crescents. These observations indicate that both proteasomal and autophagy/lysosomal degradation of ApoB occur around CLDs and that the CLD surface functions as a unique platform for convergence of the two pathways.

INTRODUCTION

Lipid droplets (CLDs) consist of a neutral lipid core with a surrounding phospholipid monolayer (Murphy and Vance, 1999; Tauchi-Sato *et al.*, 2002). CLDs are prominent in adipose cells and steroidogenic cells, but they also exist in other cell types. With the exception of a few cell types, CLDs have been considered as inert excess lipid deposits. However, recent studies have shown that a variety of proteins are localized in CLDs, suggesting that they may play more active functional roles than previously thought. In addition to PAT family proteins, enzymes involved in eicosanoid formation, enzymes for cholesterol synthesis, signaling proteins, caveolins, and Rab proteins have been reported in CLDs (Ozeki *et al.*, 2005, and references therein). Proteomic studies identified many more proteins of both known and unknown functions in the CLD-rich fraction (Brasaemle *et al.*, 2004; Fujimoto *et al.*, 2004; Liu *et al.*, 2004; Umlauf *et al.*,

2004). The presence of functional proteins implies that CLDs are not mere lipid storage vessels but may be involved in various cellular activities.

In hepatocytes, the triglycerides in CLDs are thought to be used for the synthesis of very low-density lipoprotein (VLDL) (Gibbons *et al.*, 2000). Enzyme activities that hydrolyze and reesterify neutral lipids are found in CLDs and/or endoplasmic reticulum (ER), but the detailed mechanism by which the CLD content is mobilized and incorporated into lipoprotein particles is still unclear (Murphy, 2001). Apolipoprotein B (ApoB)-100, the primary protein component of VLDL, is assembled with lipids in the ER lumen, and further lipidation and maturation of the lipoprotein particles occur in the ER or the pre-Golgi compartment (Olofsson *et al.*, 1999; Pan *et al.*, 2002). ApoB is a huge amphipathic protein of 4536 amino acids, and when the assembly of VLDL does not proceed effectively, excess ApoB molecules are destined for degradation by both proteasomal and nonproteasomal pathways (Fisher *et al.*, 1997; Cavallo *et al.*, 1999). In contrast to most other proteins subjected to ER-associated degradation, with a notable exception of major histocompatibility complex class I heavy chains in the presence of US2 or US11 (Wiertz *et al.*, 1996a,b), ApoB is ubiquitinated and transferred to proteasomes directly from the ER membrane without full translocation into the lumen (Mitchell *et al.*, 1998; Pariyarath *et al.*, 2001).

In studying the functional role of CLDs in VLDL assembly, we found serendipitously that ApoB accumulated heavily around CLDs. Subsequent experiments revealed that the ApoB accumulation around CLDs increased markedly when either proteasomal function or autophagy were

This article was published online ahead of print in *MBC in Press* (<http://www.molbiolcell.org/cgi/doi/10.1091/mbc.E05-07-0659>) on April 5, 2006.

□ The online version of this article contains supplemental material at *MBC Online* (<http://www.molbiolcell.org>).

Address correspondence to: Yuki Ohsaki (yohsaki@med.nagoya-u.ac.jp) or Toyoshi Fujimoto (tfujimot@med.nagoya-u.ac.jp).

Abbreviations used: ADRP, adipose differentiation-related protein; ALLN, *N*-acetyl-L-leuciny-L-leuciny-L-norleucinal; ApoB, apolipoprotein B; CLD, cytoplasmic lipid droplets; 3-MA, 3-methyladenine; VLDL, very low-density lipoprotein.

inhibited. Ubiquitinated ApoB, proteasomal subunits, and autophagic vacuoles were all found in or around the ApoB-positive CLDs. The observation indicates that CLDs provide a site to hold amphipathic ApoB without gross aggregation, where proteasomal and autophagic pathways converge for degradation.

MATERIALS AND METHODS

Cells and Transfection

The human hepatocellular carcinoma cell lines Huh7 and HepG2 were obtained from the Japanese Collection of Research Bioresources Cell Bank (Tokyo, Japan). They were cultured in DMEM supplemented with 10% fetal calf serum (FCS), 50 U/ml penicillin, and 0.05 mg/ml streptomycin at 37°C in a humidified atmosphere containing 5% CO₂. Frozen human hepatocytes were purchased from Tissue Transformation Technologies (Edison, NJ), and cultured in the incubation medium obtained from BIOPREDIC International (Rennes, France). When appropriate, cells were incubated in medium containing 10 μM *N*-acetyl-L-leucyl-L-leucyl-L-norleucinal (ALLN; Sigma-Aldrich, St. Louis, MO) or MG132 (Sigma-Aldrich) to inhibit proteasome functions, and/or 10 mM 3-methyladenine (3-MA; Sigma-Aldrich) to inhibit autophagy. Lipoprotein-deficient serum (LPDS) was prepared from FCS as described previously (Goldstein *et al.*, 1983).

In some experiments, cells were transfected with cDNA by using Lipofectamine 2000 (Invitrogen, Carlsbad, CA) according to the manufacturer's instruction. Expression vectors for dynamin-2 and myc/His6-tagged ubiquitin were kindly donated by Drs. Kazuhisa Nakayama (Kyoto University, Kyoto, Japan) and Ron R. Kopito (Stanford University, Stanford, CA), respectively.

Antibodies and Reagents

Mouse monoclonal anti-human ApoB-100 (clone 6H12 from INTRACEL, Frederick, MD; clone 5F8 from MONOSAN, Uden, The Netherlands), goat polyclonal anti-human ApoB-100 (Rockland, Gilbertsville, PA), mouse anti-adipose differentiation-related protein (ADRP) (Progen, Brisbane, Australia), mouse anti-ubiquitin (clone FK1; Affinity Bioreagents, Golden, CO), mouse anti-early endosomal antigen (EEA1) (Transduction Laboratories, Lexington, KY), and mouse anti-lysosomal-associated membrane protein (Lamp1) antibody (clone H4A3; Developmental Studies Hybridoma Bank, University of Iowa, Iowa City, IA) were obtained from the respective suppliers. Mouse anti-lysobisphosphatidic acid, rabbit anti-GM130, rabbit anti-ADRP, rabbit anti-LC3, and rabbit anti-polyubiquitin antibodies were kindly provided by Drs. Toshihide Kobayashi (RIKEN, Wako, Japan), Nobuhiro Nakamura (Kanazawa University, Ishikawa, Japan), Tom Keenan (Virginia Polytechnic Institute, Blacksburg, VA), Yasuo Uchiyama (Osaka University, Osaka, Japan), and Sadaki Yokota (Yamanashi University, Yamanashi, Japan), respectively. Mouse GC3α antibody recognizing α2, α6, and α7 proteasomal subunits and guinea pig anti-α6 antibodies were obtained as described previously (Tokumoto *et al.*, 1995; Wakata *et al.*, 2004). Rabbit anti-TIP47 antibody was raised against a human TIP47 peptide (residues 305-318) as reported previously (Miura *et al.*, 2002). Secondary antibodies conjugated to fluorochromes (Invitrogen, Carlsbad, CA; Jackson ImmunoResearch Laboratories, West Grove, PA), and streptavidin-colloidal gold (BioCel, Plano, Germany) were purchased from the respective suppliers. Mevastatin, mevalonolactone, brefeldin A, and rhodamine-transferrin were obtained from Sigma-Aldrich.

Subcellular Fractionation and Proteasome Activity Assay

Cells were disrupted by nitrogen cavitation and subjected to sucrose density-gradient ultracentrifugation as described previously (Fujimoto *et al.*, 2001). Absence of contamination by other organelles was confirmed by Western blotting of marker molecules as described previously (Tauchi-Sato *et al.*, 2002; Ozeki *et al.*, 2005). The proteasomal activity was assayed using 100 μM *N*-succinyl-Leu-Leu-Val-Tyr-7-amino 4-methylcoumarin (Bachem, Bubendorf, Switzerland) as the substrate according to the published protocol (Gaczynska *et al.*, 1994).

Immunoprecipitation and Western Blotting

The lipid droplet fraction obtained from the top of the sucrose density gradient was dissolved in lysis buffer (50 mM Tris, 150 mM NaCl, 1 mM EDTA, 1% NP-40, 0.5% sodium deoxycholate, 0.1% SDS, and protease inhibitor cocktail [Sigma-Aldrich], pH 8.0). Lysates were precleared using protein A-agarose (Santa Cruz Biotechnology, Santa Cruz, CA) and then incubated with 2 μg of goat anti-ApoB antibody for 8 h, followed by incubation with rabbit anti-goat IgG antibody for 2 h and then with protein A-agarose for 2 h. The agarose beads were washed in lysis buffer and bound proteins were eluted by heating at 60°C for 10 min in SDS sample buffer. All the immunoprecipitation procedure was carried out at 4°C.

In some experiments, subcellular fractions were precipitated with 10% trichloroacetic acid, dissolved in sample buffer, and subjected to Western blotting. After incubation with horseradish peroxidase-conjugated second

antibodies (Pierce Chemical, Rockford, IL), the blots were developed using Super Signal West Dura Substrate (Pierce Chemical).

Immunofluorescence Microscopy and Data Analysis

Cells were fixed with 3% formaldehyde in 0.1 M phosphate buffer for 15 min for double labeling of ApoB and organelle markers, or with a mixture of 3% formaldehyde and 0.025% glutaraldehyde in 0.1 M phosphate buffer for 15 min for double labeling of ApoB and either ADRP or TIP47. To visualize acidic organelles, cells were incubated with 500 nM LysoTracker-Red (Invitrogen) for 2 h before fixation. For immunolabeling, the fixed cells were permeabilized with 0.01% digitonin in phosphate-buffered saline (PBS) for 30 min, and treated with 3% bovine serum albumin in PBS for 10 min. The cells were then incubated for 1 h with goat or mouse anti-ApoB antibody in combination with another antibody in 1% bovine serum albumin in PBS and then with secondary antibodies for 1 h. CLDs and nuclei were stained with BODIPY493/503 (Invitrogen) and 4,6-diamidino-2-phenylindole (DAPI), respectively. Images were captured using an LSM 5 PASCAL/Axiocscope 2 laser scanning microscope or Apotome/Axiocvert 200M microscope (Carl Zeiss, Jena, Germany), using an Achromat 63× lens with a 1.40 numerical aperture. Specimens were moved in a predetermined manner along the *x-y*-axis using the mechanical stage of the microscope, and pictures were taken arbitrarily along the path. Color, brightness, and contrast of the images were adjusted using Adobe Photoshop 7.0 (Adobe Systems, Mountain View, CA). Cell numbers and colocalization of ApoB and other markers were quantified using ImageJ (<http://rsb.info.nih.gov/ij/>).

Conventional Electron Microscopy and Immunoelectron Microscopy

For conventional electron microscopy, cells cultured on coverslips were fixed with 2.5% glutaraldehyde in 0.1 M sodium cacodylate buffer, pH 7.4, post-fixed with 1% osmium tetroxide in the same buffer, stained en block with uranyl acetate, and embedded in Epon for thin sectioning. For immunoelectron microscopy, cells were fixed with 3% formaldehyde and 0.025% glutaraldehyde in 0.1 M PIPES buffer, pH 7.4, for 60 min, infiltrated with a mixture of sucrose and polyvinylpyrrolidone, and frozen in liquid nitrogen. Ultrathin cryosections were treated sequentially with goat anti-ApoB-100 antibody, biotinylated horse anti-goat IgG antibody, and streptavidin-colloidal gold (10 nm). Sections were embedded in 2% methylcellulose containing 0.3–0.5% uranyl acetate (Liou *et al.*, 1996) and observed using a JEOL 1200CX electron microscope operated at 100 kV.

RESULTS

ApoB around CLDs Is Increased by Proteasome Inhibitors

Huh7 cells are derived from human hepatoma and retain the ability to secrete VLDL (Higashi *et al.*, 2002, 2003; Lalanne *et al.*, 2005). At least 25% of ApoB in the conditioned medium was recovered as lipoproteins of <1.063 g/cm³ (our unpublished data). When Huh7 cells cultured in standard medium were labeled for ApoB, intense labeling was observed in crescent or circular shapes in occasional cells. Double labeling with BODIPY493/503 showed that the crescent-shaped or circular labeling of ApoB was localized around CLDs (Figure 1A). Based on the characteristic shape, we called the ApoB labeling around CLDs the "ApoB-crescent." ApoB-crescents were labeled in the same manner by three different antibodies to ApoB (mouse monoclonal clone 6H12 and goat polyclonal, Figure 1A; mouse monoclonal clone 5F8, our unpublished data). ApoB-crescents were also identified in another hepatoma-derived cell line, HepG2, and in primary human hepatocyte, although the frequency was lower than in Huh7 cells (Supplemental Figure 1).

The frequency of ApoB-crescents increased markedly when the cells were treated by proteasome inhibitors, ALLN or MG132. ALLN at 10 μM increased the percentage of Huh7 cells showing ApoB-crescents from <10% at 0 h to nearly 50% at 12 h (Figure 1, B and C). The ALLN treatment also increased the ratio of CLDs bearing ApoB-crescents in a similar manner (Figure 1D). The increases were significant as early as 1 h after addition of ALLN. These observations suggest that ApoB-crescents are related to the ubiquitin-proteasome degradation of ApoB. MG132 at 50 μM or ALLN at concentrations >20 μM caused a similar increase but

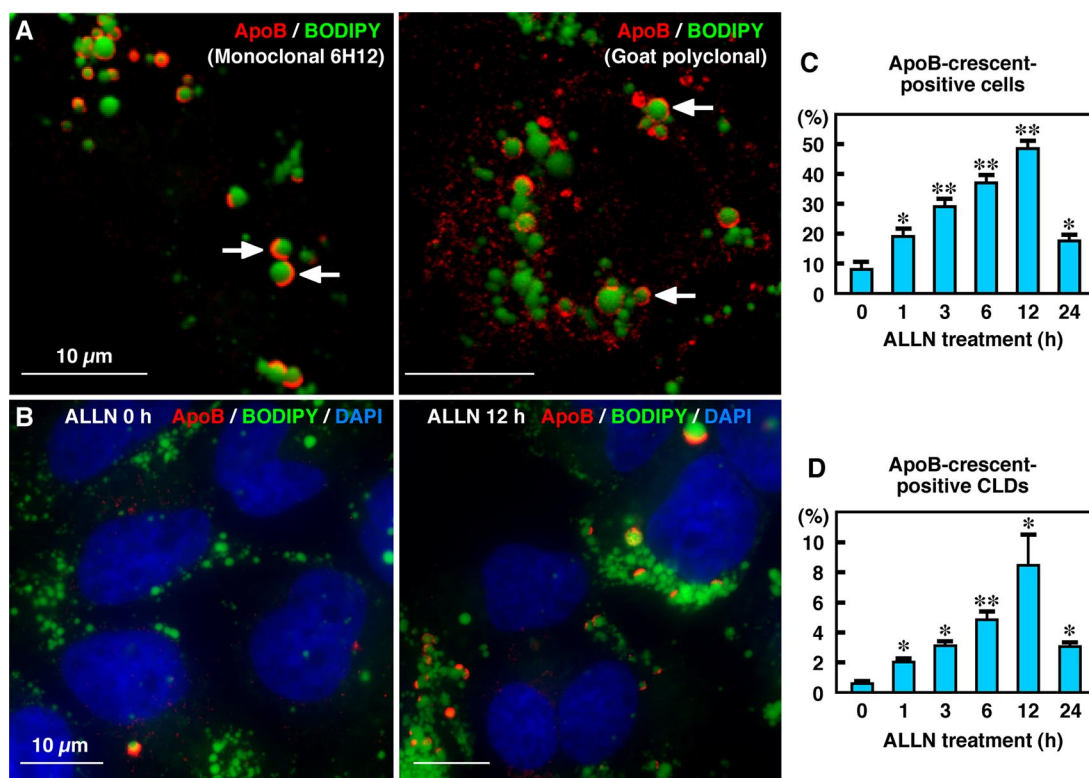


Figure 1. ApoB was localized in crescent-shaped areas adjacent to lipid droplets. (A) Huh7 cells cultured in normal medium. Some cells showed labeling for ApoB (red) in a crescent shape adjacent to lipid droplets stained by BODIPY493/503 (green). Two different anti-ApoB antibodies, mouse monoclonal (clone 6H12; left) and goat polyclonal (right), gave essentially the same results. Bars, 10 μm . (B) The crescent-shaped ApoB labeling increased markedly when Huh7 cells were treated with 10 μM ALLN for 12 h. Cell nuclei were labeled with DAPI. Bars, 10 μm . (C and D) Percentage of cells (C) and CLDs (D) showing ApoB-crescents. The frequency of crescent-positive cells and CLDs increased gradually up to 12 h by ALLN treatment and then decreased at 24 h. Results of three independent experiments were averaged; statistical difference from the control (0 h) was examined by Student's *t* test (* $p < 0.01$, ** $p < 0.001$).

affected the overall cell shape. Therefore, we mainly used 10 μM ALLN for the subsequent experiments. Notably, the frequency of ApoB-crescents decreased to the basal level after 24 h of ALLN treatment (Figure 1C), and ApoB labeling in other locations increased as described below.

The increase of ApoB-crescents was also observed when cells were cultured in DMEM with 10% LPDS instead of 10% FCS (Supplemental Figure 2). The frequency of ApoB-crescent further increased by adding mevastatin and mevalonolactone to the LPDS medium to inhibit *de novo* synthesis of cholesterol without affecting isoprenylation of Ras family proteins. Mevastatin/mevalonolactone alone also induced a slight but significant increase of ApoB-crescents. These results showed that ApoB-crescents were formed when lipid supply was not adequate and that they did not form only as a result of nonspecific stress response to the protease inhibition. Brefeldin A, which blocks vesicular transport from ER to Golgi, induced a sharp increase of ApoB-crescents as expected.

ApoB-Crescents Were Complementary to ADRP and TIP47 around CLDs

Among the PAT proteins that coat CLDs in mammalian cells, ADRP and TIP47 are expressed in nonadipocytes (Miura *et al.*, 2002; Ohsaki *et al.*, 2005; Wolins *et al.*, 2005). On immunofluorescence microscopy of Huh7 cells in the standard culture condition, ADRP was observed in most CLDs, whereas TIP47 was seen in $\sim 10\%$ of CLDs (Ohsaki *et al.*,

2005). Both ADRP and TIP47 were seen to encircle the whole surface of CLDs that lacked ApoB labeling, but where ApoB-crescents were observed, the two proteins were excluded from the ApoB-positive area (Figure 2). Vertical reconstruction of confocal images showed that CLD globules contained clear complementary ADRP/TIP47-positive and ApoB-positive hemispheres (Figure 2). By triple labeling of ApoB, ADRP, and TIP47, ADRP and TIP47 were found to coexist in those CLDs (our unpublished data). Another CLD-specific protein, Rab18 (Ozeki *et al.*, 2005), was never found in CLDs with ApoB-crescents, but it occurred in those without ApoB-crescents (our unpublished data).

CLD Fraction Contained Ubiquitinated ApoB and Proteasomal Subunits

On sucrose density-gradient centrifugation of disrupted Huh7 cells, CLDs were recovered in the top floating fraction as shown by ADRP labeling (Figure 3A). The density of ApoB-containing lipoproteins secreted from Huh7 cells was reported as 1.04–1.06 g/cm^3 (Higashi *et al.*, 2002) and that of premature lipoproteins in the secretory pathway must be no less than that, whereas the top three layers used for the CLD isolation were 0.99, 1.03, and 1.04 g/cm^3 . Thus, lipoproteins in the secretory pathway were not likely to be included in the top fraction. Markers of other organelles and soluble proteins were detected only in the bottom fractions (Lamp1 as shown in Figure 3A; Ozeki *et al.*, 2005), which confirmed

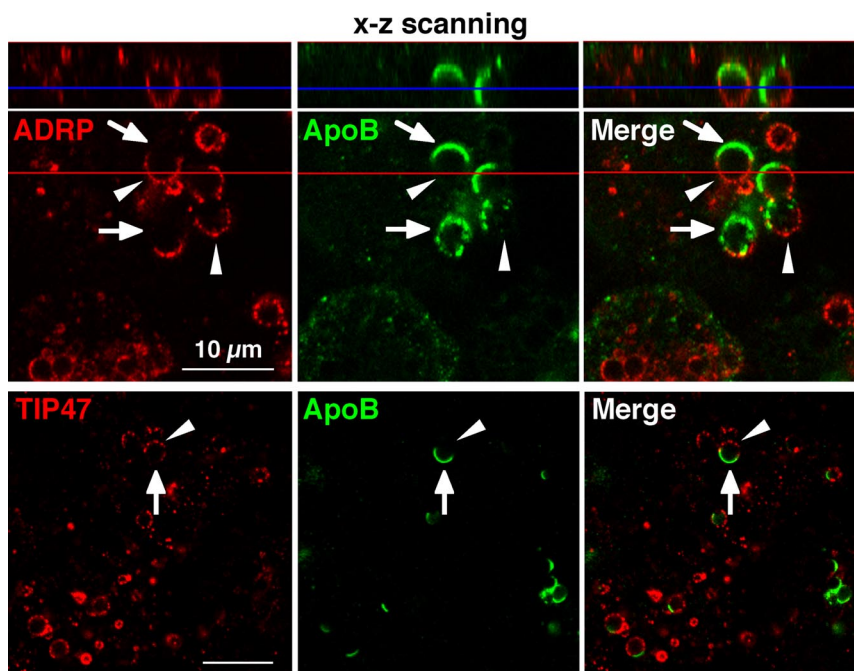


Figure 2. The crescent-shaped ApoB was complementary to ADRP and TIP47 in the CLD surface. Confocal images of ADRP (red) and ApoB (green) (top) and TIP47 (red) and ApoB (green) (bottom) in Huh7 cells treated with 10 μ M ALLN for 12 h. Images reconstructed in the x-z-axis along the red line are shown above the top panel. In most CLDs, the ApoB labeling occupied one- to two-thirds of the CLD surface (arrows), whereas both ADRP and TIP47 labeling were seen in the area complementary to the ApoB-positive area (arrowheads). Bars, 10 μ m.

the purity of the CLD fraction. ApoB was recovered in both the CLD fraction and in the bottom fractions. By measuring the reaction intensity in the Western blotting, the proportion

of ApoB in the CLD fraction increased significantly from <1% in the control to ~15% in the ALLN-treated cell (n = 3; Supplemental Figure 3).

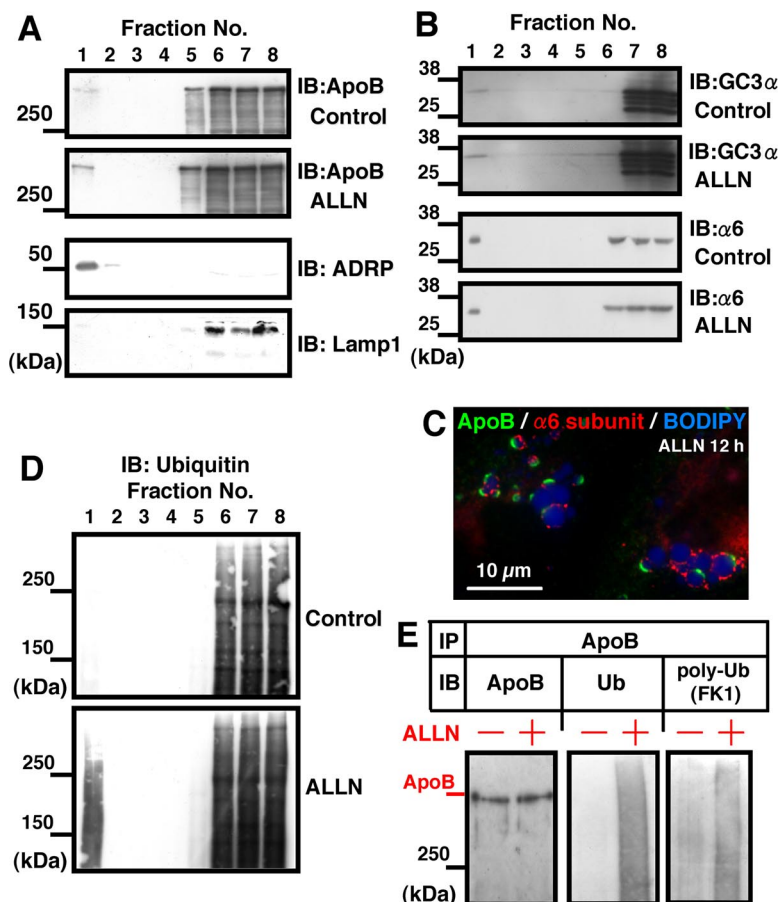


Figure 3. The CLD fraction was enriched with ApoB, proteasome subunits, and ubiquitinated proteins. (A, B, and D) Huh7 cells were cultured with or without 10 μ M ALLN for 12 h, and fractions obtained by sucrose density-gradient centrifugation were subjected to Western blotting. (A) ApoB (goat anti-ApoB antibody). Fraction 1 obtained from the top of the gradient contained ApoB and its amount was greater in the ALLN-treated sample than in the control (see Supplemental Figure 3 for quantitation). The concentration of ADRP (third panel) and the lack of Lamp1 (fourth panel) verified that the fraction was highly enriched with CLD. The result shown is representative of three independent experiments. (B) Western blotting by GC3 α and anti- α 6 antibody recognizing proteasomal subunits. The CLD fraction showed positive bands with both antibodies. (C) The proteasome subunit α 6 was localized adjacent to CLDs bearing ApoB-crescents. α 6 was also seen around CLDs that do not bear ApoB-crescents and even without ALLN treatment (our unpublished data). (D) Ubiquitin. The ubiquitinated proteins recovered in the CLD fraction were increased significantly by ALLN treatment. (E) The CLD fractions taken from control and ALLN-treated cells were adjusted to the same volume, lysed, and immunoprecipitated with goat anti-ApoB antibody. The precipitated proteins were subjected to Western blotting with anti-ApoB (left), anti-ubiquitin (middle), or anti-polyubiquitin antibodies (right). The ubiquitination of ApoB was increased significantly in the ALLN-treated sample. Cells transfected with ubiquitin cDNA were used for this experiment, but essentially the same result was obtained by using cells without the overexpression.

Immunofluorescence analyses suggested that CLDs are a site of ubiquitin-proteasome-dependent ApoB degradation. To test this assumption, we examined whether proteasome components and ubiquitinated proteins were associated with CLDs. By Western blotting, proteasome subunits were detected in the CLD fraction (Figure 3B); by densitometry, the amount of GC3 α -reactive bands in the CLD fraction (fraction 1) was estimated to be \sim 0.23% of the fraction 8, containing the cytosol. Moreover, by immunofluorescence microscopy, α 6 was found around CLDs adjacent to apoB-crescents (Figure 3C). The proteasomal activity of the isolated CLD fraction was 0.18% of the fraction 8, but it was likely to be underestimated because turbidity caused by lipid esters disturbed the measurement significantly (Supplemental Figure 4). Ubiquitinated proteins in the CLD fraction were also increased drastically by ALLN (Figure 3D). Finally, ApoB in the CLD fraction immunoprecipitated by an anti-ApoB antibody showed ubiquitination, and the degree of ubiquitination increased after ALLN treatment (Figure 3E). These observations indicate that CLDs of Huh7 cells are associated with proteasomes and ubiquitinated proteins, including ApoB, and their amount increases when the proteasomal function is inhibited.

ApoB-positive Electron-lucent Particles Clustered Next to CLDs

To elucidate the identity of ApoB-crescents, Huh7 cells were observed by conventional electron microscopy. In untreated control cells, CLDs were observed as round lucent structures, and their perimeter was demarcated from the cytoplasmic matrix (Figure 4A). After ALLN treatment, CLDs themselves were observed similarly, but they were frequently associated with a cluster of small electron-lucent particles (Figure 4B, arrows). Some small particles ranging in diameter from 50 to 100 nm were observed apart from CLDs, but most were seen to be in contact with CLDs. On immunogold labeling of ultrathin cryosections, electron-lucent areas next to CLDs were seen to be labeled strongly for ApoB (Figure 4C, arrows). In cryosections, demarcation between particles was not clear, probably due to the difference in the staining procedures, but ApoB labeling most likely occurred around the small particles adjacent to CLDs. Interestingly, the contents of CLDs and the small particles often showed different electron densities in both Epon sections and cryosections, indicating some compositional differences between them (Figure 4, B and C). The above-mentioned observations suggested that clusters of small lucent particles adjacent to CLDs were the ApoB-crescents observed by immunofluorescence microscopy.

ApoB Is Increased in Lysosomes by ALLN

Immunofluorescence labeling revealed that ApoB was localized to structures other than CLDs. In addition to diffuse labeling in the cytoplasm that probably corresponded to the ER, labeling was observed in distinct dots that were not related to BODIPY493/503 staining. The latter dot-type labeling increased after ALLN treatment (Figure 5A, arrows). On double labeling with various organelle markers, ApoB labeling hardly overlapped with either GM130, a Golgi marker, or EEA1, an early endosome marker (Figure 5B). In contrast, ApoB labeling colocalized extensively with late endosome/lysosome markers Lamp1 and lysobisphosphatidic acid (our unpublished data), and Lysotracker, an acidic organelle marker (Figure 5C). Compared with untreated cells, colocalization of ApoB and Lysotracker was increased by \sim 2.5-fold after 6 h of ALLN treatment and increased further to more than fivefold at 24 h (Figure 5D). The time

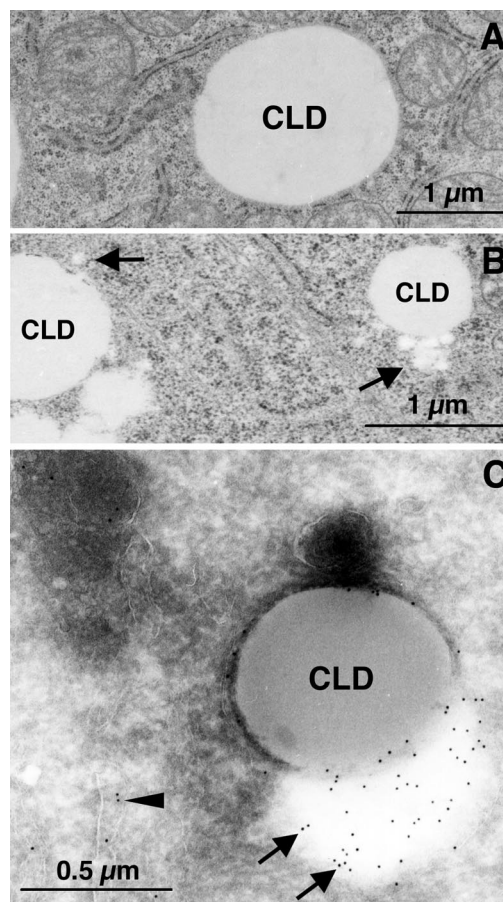


Figure 4. ApoB-positive low-density particles occurred adjacent to CLD in ALLN-treated Huh7 cells. (A and B) Huh7 cells were cultured with or without 10 μ M ALLN for 12 h and observed by conventional electron microscopy. In control cells (A), the rim of CLDs was demarcated by the cytoplasm. In ALLN-treated cells (B), CLDs were often associated with a cluster of small round electron-lucent particles (arrows). The small particles ranged from 50 to 100 nm in diameter. Bars, 1 μ m. (C) Immunogold labeling of ApoB in Huh7 cells treated with 10 μ M ALLN for 12 h. ApoB was localized to the electron-lucent particles adjacent to CLDs (arrows). The electron density of the ApoB-positive particles was lower than that of CLDs, implying a difference in their composition. ApoB labeling was also seen in the ER lumen (arrowheads). Bar, 0.5 μ m.

course was different from that of the frequency of ApoB-crescents that decreased rapidly after 12 h of ALLN treatment (compare Figures 1C and 5D).

Immunogold labeling of cryosections revealed that the lysosomal lumen contained electron-lucent components labeled for ApoB (Figure 5E, arrows). Interestingly, the lysosomes were usually seen in the vicinity of ApoB-crescents adjacent to CLD. In some cases, the limiting membrane of the lysosomes containing ApoB labeling seemed to wrap around the ApoB-crescent and the adjacent CLD (Figure 5F).

The absence of ApoB in the early endosome (Figure 5B) implied that the lysosomal ApoB was not derived from endocytosed VLDL. To further confirm this point, cDNA of dominant-negative dynamin-2 (K44A) was transfected, and its effect on the amount of the lysosomal ApoB was examined. In comparison with wild-type dynamin-2, the K44A mutant inhibited the uptake of rhodamine-transferrin, but it did not affect the apoB labeling that colocalized with Lyso-

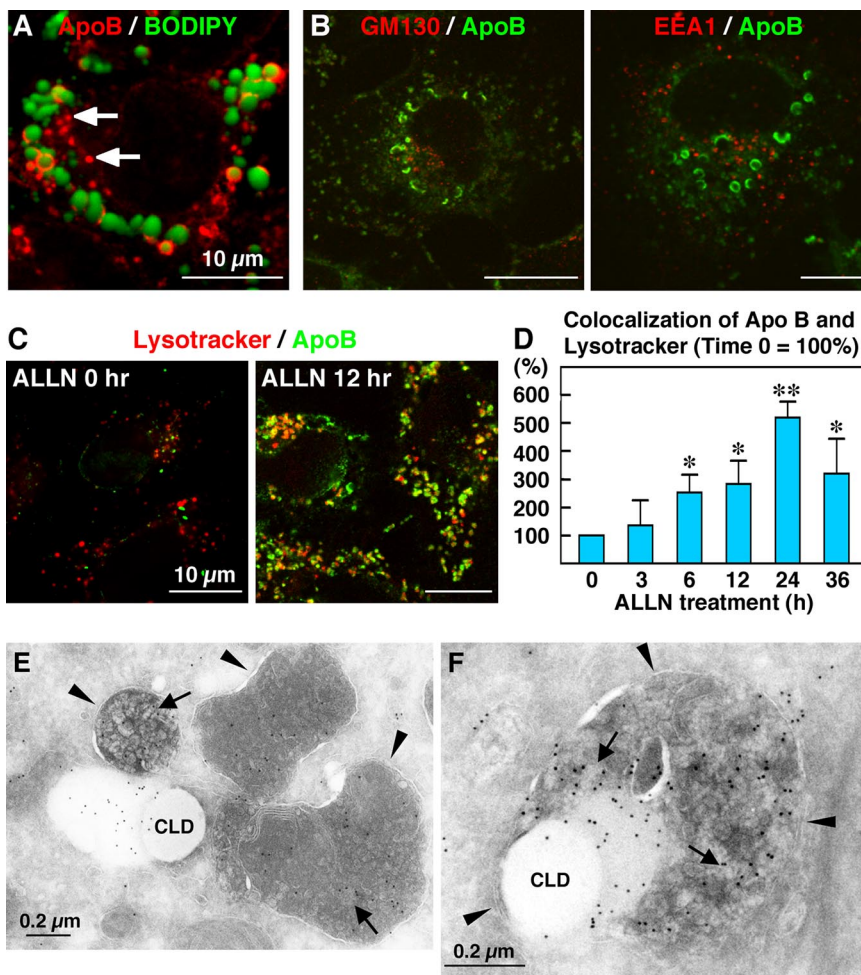


Figure 5. ApoB in lysosomal structures was increased by ALLN treatment. Bars, 10 μm . (A and B) Huh7 cells treated with 10 μM ALLN for 12 h. Many ApoB-positive structures were not colocalized with BODIPY493/503 (arrows in A), GM130 (B-left), or EEA1 (B-right). (C) Colocalization of ApoB (green) and Lysotracker (red) increased drastically after ALLN treatment. (D) Huh7 cells treated with 10 μM ALLN for the indicated times were incubated with 500 nM Lysotracker-Red for 2 h before fixation and immunolabeling. Colocalization of ApoB and Lysotracker-Red was quantified by measuring the number of double-positive pixels in confluent cells. Results of three independent experiments were averaged; statistical difference from the control (0 h) was examined by Student's *t* test (* $p < 0.05$, ** $p < 0.001$). (E and F) Immunogold labeling of ALLN-treated Huh7 cells. Bars, 0.2 μm . (E) Lysosomes (arrowheads) contained ApoB-positive electron-lucent particles (arrows) and adhered to the ApoB-crescent area adjacent to CLDs. (F) In some cases, the lysosomes containing ApoB labeling (arrows) wrapped around the ApoB-crescent and the adjacent CLD. The limiting membrane of the lysosome is marked by arrowheads.

tracker (Supplemental Figure 5). The result showed that most ApoB in the lysosome was not caused by uptake of the secreted lipoprotein.

ApoB-Crescents Are Processed by Autophagy

The above-mentioned result as well as immunoelectron microscopy of ALLN-treated cells suggested that the ApoB-positive particles in the lysosome were largely caused by autophagy. In fact, a previous study demonstrated that inhibition of proteasomes in Huh7 cells induced autophagic vacuoles (Harada *et al.*, 2003). The increase in autophagic vacuoles was confirmed by labeling with LC3 (Kabeya *et al.*, 2000); by ALLN treatment, the increase of LC3-positive particles was already evident at 1 h and became drastic at 12 h (Figure 6A and Supplemental Figure 6). By triple labeling for ApoB, LC3, and neutral lipids, the LC3-positive autophagosomes were often seen adjacent to ApoB-crescents (Figure 6B, arrows). By treating the cells with leupeptin for 30 min to inhibit the lysosomal digestion, ApoB-crescents in the Lamp1-positive organelles were detected (Figure 6C, arrow). These observations suggest that inhibition of proteasomal function induced autophagic vacuoles, which may then engulf ApoB-crescents and adjacent CLDs. The decrease in ApoB-crescents after 12 h of ALLN treatment indicated that autophagy was activated to a sufficient degree by that time.

The above-mentioned assumption was tested by inhibiting autophagy by 3-MA. The ALLN-induced increase in LC3

was suppressed when the medium contained 10 mM 3-MA (Figure 6A), which confirmed the effectiveness of the reagent. In cells treated with 3-MA at 12 h after the beginning of ALLN treatment, the decrease in ApoB-crescents between 12 and 24 h was suppressed (Figure 6D). The suppressive effect was more obvious when cells were treated with 3-MA and ALLN from the beginning (Figure 6D). This observation verified that autophagy is important in the processing of ApoB-crescents. Furthermore, it suggested that even when proteasomal function is normal, autophagy may function in ApoB degradation. This assumption proved correct because 3-MA alone caused an increase in ApoB-crescent-positive cells and CLDs (Figure 6, E and F). The ratio of ApoB-crescent-positive cells increased to more than 30% at 12 h after addition of 3-MA. The results of the present study indicate that proteasomal and autophagocytic systems collaborate to process ApoB and that CLDs provide a site at which the two degradation systems converge.

DISCUSSION

CLDs as Sites of Proteasomal Processing of ApoB

ApoB is the primary structural protein of VLDL. It is synthesized on membrane-bound ribosomes and translocated to the ER lumen cotranslationally. Nascent lipoprotein particles are first assembled in the rough ER, and after maturation in the smooth ER and possibly in the Golgi, they are

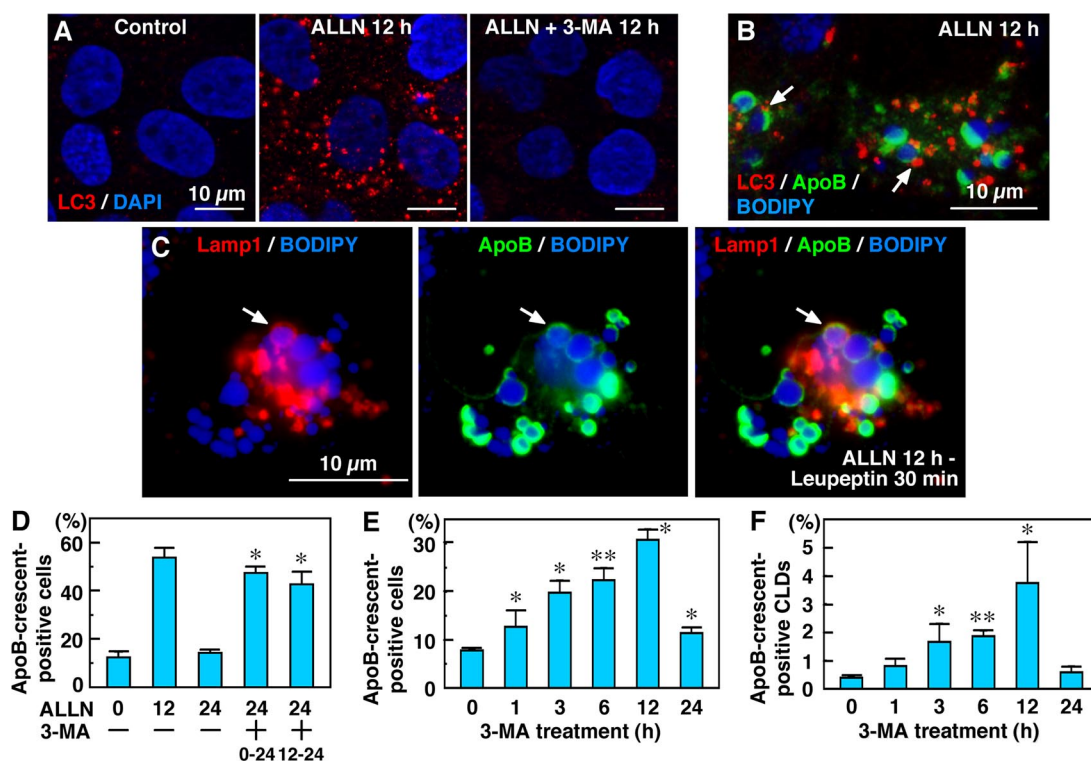


Figure 6. Autophagy is involved in processing the ApoB-crescent. (A) LC3 was observed only infrequently in Huh7 cells cultured under normal conditions. ALLN (10 μ M; 12 h) increased LC3 markedly, but cotreatment with 10 mM 3-MA suppressed the increase. Cell nuclei were labeled by DAPI. Bars, 10 μ m. (B) Triple labeling for LC3 (red), ApoB (green), and BODIPY493/503 (blue) in ALLN-treated cells. LC3 was seen near the ApoB-crescent and its adjacent CLD (arrows). Bar, 10 μ m. (C) Triple labeling for Lamp1 (red), ApoB (green), and BODIPY493/503 (blue). Cells were cultured with 10 μ M ALLN for 12 h and added with 100 μ M leupeptin for 30 min. The ApoB-crescent and the adjacent CLD was found in the Lamp1-positive late endosome/lysosome (arrow). (D) In comparison with cells cultured with ALLN alone for 24 h, addition of 3-MA at 0 h or 12 h increased the ratio of ApoB-crescent-positive cells at 24 h. The difference was statistically significant by Student's *t* test ($n = 3$; * $p < 0.001$). (E and F) Percentage of cells (E) and CLDs (F) showing ApoB-crescents in cells treated with 3-MA alone. The frequency of crescent-positive cells and CLDs reached a maximum at 12 h. Results of three independent experiments were averaged; statistical difference from the control (0 h) was examined by Student's *t* test (E: * $p < 0.01$, ** $p < 0.001$; F: $p < 0.05$, ** $p < 0.001$).

secreted by exocytosis (for review, see Davis 1999). Thus, along with other secretory proteins, ApoB has been shown to exist in the ER and Golgi (Sakata *et al.*, 2001). In addition, labeling for ApoB was also observed in lysosomes (Du *et al.*, 1998), which may be derived, at least partially, from secreted and then endocytosed VLDL (Williams *et al.*, 1990; Twisk *et al.*, 2000). However, to our knowledge, there have been no previous reports of localization of ApoB on the CLD surface. The cluster of ApoB-positive particles adjacent to CLDs, which we designated the "ApoB-crescent," was observed in both Huh7 and HepG2 cells and increased markedly when proteasome function was inhibited. In HepG2 cells, inhibition of proteasomes was reported to cause particulate accumulation of ApoB in association with the ER, but the ApoB-crescent was not described (Fisher *et al.*, 1997; Pariyatharath *et al.*, 2001). ApoB-crescent may not have been identified previously because of its relatively low frequency in HepG2 cells. Furthermore, without CLD staining, it may be difficult to discriminate between ApoB-crescents and dense particulate labeling.

Degradation of ApoB has been reported to occur by both proteasomal and nonproteasomal pathways (Cavallo *et al.*, 1999; Fisher *et al.*, 2001). When conditions are not appropriate for VLDL assembly, ubiquitination and proteasomal degradation of ApoB increase. In contrast to most other proteins that probably undergo retrotranslocation from the ER lumen for ER-associated degradation, ApoB is thought to

remain halfway through the translocon before being extracted to the cytoplasm for degradation (Fisher and Ginsberg, 2002); thus, proteasomes where ApoB is degraded are likely to be in the proximity of the ER. In the present study, we showed that proteasome subunits are located near CLDs. CLDs are generally distributed in the proximity of the ER (Murphy and Vance, 1999), and lipids stored in CLDs are thought to be mobilized for pre-VLDL assembly in synchronization with ApoB translation (Gibbons *et al.*, 2000). This functional relationship should require that CLDs and the translocons for ApoB synthesis exist in proximity. Thus, CLDs are likely to be in the vicinity of both the ApoB translation site and proteasomes, which location seems suitable to harbor ubiquitinated ApoB for proteasomal degradation.

In addition to proximity, the CLD surface may offer another important advantage for the processing of ApoB. That is, even if the proteasomes are highly efficient in degrading multiubiquitinated proteins, there is a danger that proteins to be degraded may form aggregates in the cytoplasm through hydrophobic interactions (Kopito, 2000). Such aggregates were shown to impair proteasomal processing (Bence *et al.*, 2001) and may become toxic to the cells. In this respect, CLDs may provide a surface to hold large amphipathic proteins, such as ApoB, in an appropriate conformation and prevent them forming aggregates. This assumption is supported by the structural resemblance of CLDs and lipoprotein particles in that both consist of a neutral lipid

core and a phospholipid monolayer. The importance of the CLD surface for ApoB degradation might be tested by manipulating the expression of CLD-related proteins.

The Relationship between CLDs and Electron-lucent Particles in the ApoB-Crescent

Immunoelectron microscopy indicated that ApoB was localized around small electron-lucent particles that clustered around CLDs. Their appearance suggested that the particles are lipidic in nature, but their electron density often looked different from that of CLDs, suggesting that the contents of the particles and CLDs are not the same. The electron-lucent particles in the ApoB-crescent were 50–100 nm in diameter, roughly matching that of VLDL and/or premature VLDL (Murphy, 2001; Swift *et al.*, 2001). The origin of the particles is not known, but one possibility is that binding of ApoB induced segmentation of CLDs solely depending on the molecular nature of ApoB, and gave rise to particles of that size (Segrest *et al.*, 2001). Alternatively, lipid esters made in the ER membrane may bud to the cytoplasmic side; in this case, the particles are thought to be an aberrant form of CLDs coated with ApoB instead of PAT proteins. Finally, as a third possibility, the particles could be VLDL and/or pre-VLDL particles themselves. It is difficult to explain how they could extravasate from the luminal side, but lipidic particles bearing apolipoproteins can exist in the cytoplasm (Ito *et al.*, 2002).

In CLDs associated with ApoB-crescents, ADRP and TIP47 were seen only in the area complementary to the crescent. This distribution was reminiscent of the displacement of ADRP from CLDs when Rab18 was overexpressed (Ozeki *et al.*, 2005), which then induced close apposition of CLDs and the ER-derived membrane. The ApoB-crescent is different from the above-mentioned case in that Rab18 was not up-regulated (our unpublished data) and that both ADRP and TIP47 were expelled from the area apposing the ApoB-crescent. The function of ADRP (and possibly TIP47) may be to shield the CLD surface from other organelles (Ozeki *et al.*, 2005). The absence of PAT proteins may be necessary for the adherence of lipidic particles to CLDs and the formation of the ApoB-crescent.

Convergence of Ubiquitin-Proteasome Pathway and Autophagy-Lysosome Pathway in CLDs

ApoB level in the lysosome was increased by inhibition of the proteasome, and it persisted even after the frequency of ApoB-crescents began to decrease after 12 h. Two different mechanisms have been proposed to explain the existence of ApoB in the lysosome. One was the reuptake of secreted VLDL through LDL receptors (Williams *et al.*, 1990; Twisk *et al.*, 2000). The reuptake may also occur in Huh7 cells, but it is likely to be of minor importance because the lysosomal ApoB labeling persisted even in cell expressing the dominant-negative dynamin-2. The other was the proteasomal processing of ApoB resulting in a single-pass transmembrane protein (Du *et al.*, 1998). However, labeling for ApoB was observed throughout the lysosomal lumen in our immunoelectron microscopic study, which was unlikely to be caused by a transmembrane protein in the limiting membrane.

The ALLN-induced increase in ApoB in the lysosome was probably caused by autophagy. First, LC3, a specific marker of the autophagosomal membrane (Kabeya *et al.*, 2000), was increased by ALLN and was found near the ApoB-crescent. Second, electron microscopy showed autophagic structures engulfing the ApoB-crescent, and ApoB in the lysosomal lumen was found around small electron-lucent particles re-

sembling those in the ApoB-crescent. Third, the decrease in ApoB-crescents between 12 and 24 h of ALLN treatment was blocked by 3-MA, an inhibitor of autophagy. These results suggest that the ApoB-crescents were subjected to autophagy when the proteasome function was inhibited. Previously, ALLN treatment was shown to induce ubiquitin-rich intermediate filament inclusion bodies in Huh7 cells, which were removed by autophagic vacuoles (Harada *et al.*, 2003). In view of the close relationship of CLDs with intermediate filaments (Franke *et al.*, 1987; Almahbobi, 1995), it is likely that the inclusion bodies contain CLDs and the adhering ApoB-crescents.

The participation of autophagy in processing ApoB is not apparently limited to conditions where the proteasomal function is compromised. Inhibition of autophagy caused a similar increase in ApoB-crescent frequency as inhibition of the proteasome. This observation suggests that autophagy plays a major role in degradation of ApoB in Huh7 cells. Previously, autophagy was shown to process aggresomes in Schwann cells (Fortun *et al.*, 2003). More recently, using Atg7-deficient mice, ubiquitinated proteins were shown to aggregate even in the presence of functional proteasomes, and the aggregates were shown to be eliminated by the autophagic process (Komatsu *et al.*, 2005). Notably, the accumulation of ubiquitinated proteins was observed around CLDs. The authors proposed that ubiquitination may serve as a signal for the autophagic process as well as to the proteasome pathway. The results of the present study fit well with their proposal and show that such a mechanism works physiologically to process ubiquitinated proteins *in vivo*. In contrast, the relative importance of the proteasomal and autophagic pathways for the ApoB degradation may not be the same in different cell lines. For example, in HepG2 cells, a significant increase of ApoB-crescents were observed by ALLN, but not by 3-MA (our unpublished data). In the present study, Huh7 cells were used because the cell line retains the ability to secrete VLDL (Higashi *et al.*, 2002, 2003; Lalanne *et al.*, 2005), whereas HepG2 cells require exogenous fatty acids for the secretion due to the deficiency of triacylglycerol hydrolase (Lehner *et al.*, 1999). But it does not mean that other physiological mechanisms to regulate ApoB are preserved in Huh7 cells as well. The detailed degradation

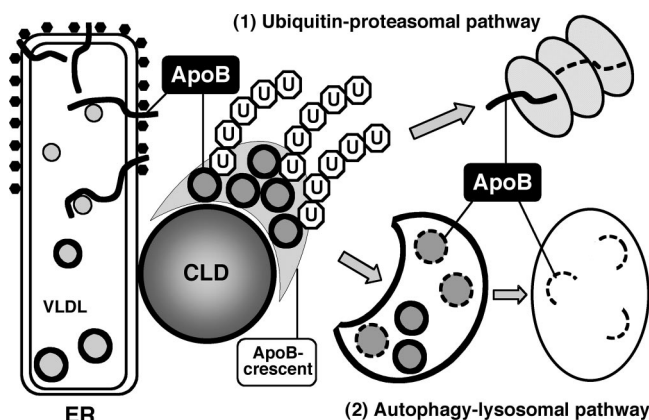


Figure 7. Role of CLDs in ApoB degradation. CLDs exist in the vicinity of the ER and may serve to hold ApoB-positive lipidic particles as the ApoB-crescent. Both the ubiquitin-proteasome pathway and the autophagy-lysosomal pathway are involved in the degradation of ApoB in normal cells. The ApoB-crescent is thought to be the site where the two degradation systems converge.

mechanism of ApoB *in vivo* needs to be studied under physiological settings.

A diagram depicting the major features of the ApoB degradation in Huh7 cells is shown in Figure 7. CLDs are likely to provide a surface to integrate the two degradation systems—proteasomal and lysosomal—for ApoB. The unique structure of CLDs must be important for their role as discussed above. In this way, CLDs in hepatocytes may act not only as a reservoir of lipids for VLDL formation but also as a platform on which to process the unused ApoB effectively, and to prevent the unusually large amphipathic molecules from forming toxic aggregates. An intriguing possibility is that the role of CLDs as a site of convergence of proteasomal and autophagic processing may not be limited to ApoB but may be extended to other amphipathic/hydrophobic proteins. In this context, it is noteworthy that oligomers of α -synuclein have a propensity to bind CLDs (Cole *et al.*, 2002). α -Synuclein is a component of intraneuronal inclusion bodies that are found in a number of neurodegenerative diseases, including Parkinson's disease (Spillantini *et al.*, 1998). In the neuronal cell, CLDs are scarce and labeling for ADRP is not observed (Heid *et al.*, 1998). If CLDs are important for the safe processing of aggregation-prone proteins, the paucity of CLDs may explain why toxic aggregates are formed preferentially in neuronal cells. Further studies to determine whether manipulation of CLD proteins and lipids would modify aggregate formation are warranted.

ACKNOWLEDGMENTS

We thank Drs. Kazuhisa Nakayama, Ron R. Kopito, Toshihide Kobayashi, Nobuhiro Nakamura, Tom Keenan, Yasuo Uchiyama, and Sadaki Yokota for providing vectors and antibodies. We are also grateful to Dr. Shigeo Murata for invaluable advice on the proteasomal activity assay and to Kumi Tauchi-Sato and Tetsuo Okumura for technical assistance. This work was supported by Grants-in-Aid for Scientific Research and the 21st Century COE Program "Integrated Molecular Medicine for Neuronal and Neoplastic Disorders" of the Ministry of Education, Culture, Sports, Science and Technology of the Japanese Government.

REFERENCES

Almahbobi, G. (1995). Adhesion of intermediate filaments and lipid droplets in adrenal cells studied by field emission scanning electron microscopy. *Cell Tissue Res.* *281*, 387–390.

Bence, N. F., Sampat, R. M., and Kopito, R. R. (2001). Impairment of the ubiquitin-proteasome system by protein aggregation. *Science* *292*, 1552–1555.

Brasaemle, D. L., Dolios, G., Shapiro, L., and Wang, R. (2004). Proteomic analysis of proteins associated with lipid droplets of basal and lipolytically stimulated 3T3-L1 adipocytes. *J. Biol. Chem.* *279*, 46835–46842.

Cavallo, D., Rudy, D., Mohammadi, A., Macri, J., and Adeli, K. (1999). Studies on degradative mechanisms mediating post-translational fragmentation of apolipoprotein B and the generation of the 70-kDa fragment. *J. Biol. Chem.* *274*, 23135–23143.

Cole, N. B., Murphy, D. D., Grider, T., Rueter, S., Brasaemle, D., and Nussbaum, R. L. (2002). Lipid droplet binding and oligomerization properties of the Parkinson's disease protein α -synuclein. *J. Biol. Chem.* *277*, 6344–6352.

Davis, R. A. (1999). Cell and molecular biology of the assembly and secretion of apolipoprotein B-containing lipoproteins by the liver. *Biochim. Biophys. Acta* *1440*, 1–31.

Du, X., Stoops, J. D., Mertz, J. R., Stanley, C. M., and Dixon, J. L. (1998). Identification of two regions in apolipoprotein B100 that are exposed on the cytosolic side of the endoplasmic reticulum membrane. *J. Cell Biol.* *141*, 585–599.

Fisher, E. A., and Ginsberg, H. N. (2002). Complexity in the secretory pathway: the assembly and secretion of apolipoprotein B-containing lipoproteins. *J. Biol. Chem.* *277*, 17377–17380.

Fisher, E. A., Pan, M., Chen, X., Wu, X., Wang, H., Jamil, H., Sparks, J. D., and Williams, K. J. (2001). The triple threat to nascent apolipoprotein B. Evidence for multiple, distinct degradative pathways. *J. Biol. Chem.* *276*, 27855–27863.

Fisher, E. A., Zhou, M., Mitchell, D. M., Wu, X., Omura, S., Wang, H., Goldberg, A. L., and Ginsberg, H. N. (1997). The degradation of apolipoprotein B100 is mediated by the ubiquitin-proteasome pathway and involves heat shock protein 70. *J. Biol. Chem.* *272*, 20427–20434.

Fortun, J., Dunn, W. A., Jr., Joy, S., Li, J., and Notterpek, L. (2003). Emerging role for autophagy in the removal of aggregates in Schwann cells. *J. Neurosci.* *23*, 10672–10680.

Franke, W. W., Hergt, M., and Grund, C. (1987). Rearrangement of the vimentin cytoskeleton during adipose conversion: formation of an intermediate filament cage around lipid globules. *Cell* *49*, 131–141.

Fujimoto, T., Kogo, H., Ishiguro, K., Tauchi, K., and Nomura, R. (2001). Caveolin-2 is targeted to lipid droplets, a new "membrane domain" in the cell. *J. Cell Biol.* *152*, 1079–1085.

Fujimoto, Y., Itabe, H., Sakai, J., Makita, M., Noda, J., Mori, M., Higashi, Y., Kojima, S., and Takano, T. (2004). Identification of major proteins in the lipid droplet-enriched fraction isolated from the human hepatocyte cell line HuH7. *Biochim. Biophys. Acta* *1644*, 47–59.

Gaczynska, M., Rock, K. L., Spies, T., and Goldberg, A. L. (1994). Peptidase activities of proteasomes are differentially regulated by the major histocompatibility complex-encoded genes for LMP2 and LMP7. *Proc. Natl. Acad. Sci. USA* *91*, 9213–9217.

Gibbons, G. F., Islam, K., and Pease, R. J. (2000). Mobilisation of triacylglycerol stores. *Biochim. Biophys. Acta* *1483*, 37–57.

Goldstein, J. L., Basu, S. K., and Brown, M. S. (1983). Receptor-mediated endocytosis of low-density lipoprotein in cultured cells. *Methods Enzymol.* *98*, 241–260.

Harada, M., *et al.* (2003). Proteasome inhibition induces inclusion bodies associated with intermediate filaments and fragmentation of the Golgi apparatus. *Exp. Cell Res.* *288*, 60–69.

Heid, H. W., Moll, R., Schwetlick, I., Rackwitz, H. R., and Keenan, T. W. (1998). Adipophilin is a specific marker of lipid accumulation in diverse cell types and diseases. *Cell Tissue Res.* *294*, 309–321.

Higashi, Y., Itabe, H., Fukase, H., Mori, M., Fujimoto, Y., Sato, R., Imanaka, T., and Takano, T. (2002). Distribution of microsomal triglyceride transfer protein within sub-endoplasmic reticulum regions in human hepatoma cells. *Biochim. Biophys. Acta* *1581*, 127–136.

Higashi, Y., Itabe, H., Fukase, H., Mori, M., Fujimoto, Y., and Takano, T. (2003). Transmembrane lipid transfer is crucial for providing neutral lipids during very low density lipoprotein assembly in endoplasmic reticulum. *J. Biol. Chem.* *278*, 21450–21458.

Ito, J., Nagayasu, Y., Kato, K., Sato, R., and Yokoyama, S. (2002). Apolipoprotein A-I induces translocation of cholesterol, phospholipid, and caveolin-1 to cytosol in rat astrocytes. *J. Biol. Chem.* *277*, 7929–7935.

Kabaya, Y., Mizushima, N., Ueno, T., Yamamoto, A., Kirisako, T., Noda, T., Kominami, E., Ohsumi, Y., and Yoshimori, T. (2000). LC3, a mammalian homologue of yeast Apg8p, is localized in autophagosomal membranes after processing. *EMBO J.* *19*, 5720–5728.

Komatsu, M., *et al.* (2005). Impairment of starvation-induced and constitutive autophagy in Atg7-deficient mice. *J. Cell Biol.* *169*, 425–434.

Kopito, R. R. (2000). Aggregosomes, inclusion bodies and protein aggregation. *Trends Cell Biol.* *10*, 524–530.

Lalanne, F., *et al.* (2005). Wild-type PCSK9 inhibits LDL clearance but does not affect apoB-containing lipoprotein production in mouse and cultured cells. *J. Lipid Res.* *46*, 1312–1319.

Lehner, R., Cui, Z., and Vance, D. E. (1999). Subcellular localization, developmental expression and characterization of a liver triacylglycerol hydrolase. *Biochem. J.* *338*, 761–768.

Liou, W., Geuze, H. J., and Slot, J. W. (1996). Improving structural integrity of cryosections for immunogold labeling. *Histochem. Cell Biol.* *106*, 41–58.

Liu, P., Ying, Y., Zhao, Y., Mundy, D. I., Zhu, M., and Anderson, R. G. (2004). Chinese hamster ovary K2 cell lipid droplets appear to be metabolic organelles involved in membrane traffic. *J. Biol. Chem.* *279*, 3787–3792.

Mitchell, D. M., Zhou, M., Pariyathar, R., Wang, H., Aitchison, J. D., Ginsberg, H. N., and Fisher, E. A. (1998). Apolipoprotein B100 has a prolonged interaction with the translocon during which its lipidation and translocation change from dependence on the microsomal triglyceride transfer protein to independence. *Proc. Natl. Acad. Sci. USA* *95*, 14733–14738.

Miura, S., Gan, J. W., Brzostowski, J., Parisi, M. J., Schultz, C. J., Londos, C., Oliver, B., and Kimmel, A. R. (2002). Functional conservation for lipid storage droplet association among Perilipin, ADRP, and TIP47 (PAT)-related proteins in mammals, *Drosophila*, and *Dictyostelium*. *J. Biol. Chem.* *277*, 32253–32257.

- Murphy, D. J. (2001). The biogenesis and functions of lipid bodies in animals, plants and microorganisms. *Prog. Lipid Res.* 40, 325–438.
- Murphy, D. J., and Vance, J. (1999). Mechanisms of lipid-body formation. *Trends Biochem. Sci.* 24, 109–115.
- Ohsaki, Y., Maeda, T., and Fujimoto, T. (2005). Fixation and permeabilization protocol is critical for immunolabeling of lipid droplet protein. *Histochem. Cell Biol.* 124, 445–452.
- Olofsson, S. O., Asp, L., and Boren, J. (1999). The assembly and secretion of apolipoprotein B-containing lipoproteins. *Curr. Opin. Lipidol.* 10, 341–346.
- Ozeki, S., Cheng, J.-L., Tauchi-Sato, K., Hatano, N., Taniguchi, H., and Fujimoto, T. (2005). Rab18 localizes to lipid droplets and induces their close apposition to the endoplasmic reticulum-derived membrane. *J. Cell Sci.* 118, 2601–2611.
- Pan, M., Liang, J. S., Fisher, E. A., and Ginsberg, H. N. (2002). The late addition of core lipids to nascent apolipoprotein B100, resulting in the assembly and secretion of triglyceride-rich lipoproteins, is independent of both microsomal triglyceride transfer protein activity and new triglyceride synthesis. *J. Biol. Chem.* 277, 4413–4421.
- Pariyath, R., Wang, H., Aitchison, J. D., Ginsberg, H. N., Welch, W. J., Johnson, A. E., and Fisher, E. A. (2001). Co-translational interactions of apolipoprotein B with the ribosome and translocon during lipoprotein assembly or targeting to the proteasome. *J. Biol. Chem.* 276, 541–550.
- Sakata, N., Phillips, T. E., and Dixon, J. L. (2001). Distribution, transport, and degradation of apolipoprotein B-100 in HepG2 cells. *J. Lipid Res.* 42, 1947–1958.
- Segrest, J. P., Jones, M. K., De Loof, H., and Dashti, N. (2001). Structure of apolipoprotein B-100 in low density lipoproteins. *J. Lipid Res.* 42, 1346–1367.
- Spillantini, M. G., Crowther, R. A., Jakes, R., Hasegawa, M., and Goedert, M. (1998). alpha-Synuclein in filamentous inclusions of Lewy bodies from Parkinson's disease and dementia with Lewy bodies. *Proc. Natl. Acad. Sci. USA* 95, 6469–6473.
- Swift, L. L., Valyi-Nagy, K., Rowland, C., and Harris, C. (2001). Assembly of very low density lipoproteins in mouse liver: evidence of heterogeneity of particle density in the Golgi apparatus. *J. Lipid Res.* 42, 218–224.
- Tauchi-Sato, K., Ozeki, S., Houjou, T., Taguchi, R., and Fujimoto, T. (2002). The surface of lipid droplets is a phospholipid monolayer with a unique Fatty Acid composition. *J. Biol. Chem.* 277, 44507–44512.
- Tokumoto, T., Yamashita, M., Yoshikuni, M., Kajiura, H., and Nagahama, Y. (1995). Purification of latent proteasome (20S proteasome) and demonstration of active proteasome in goldfish (*Carassius auratus*) oocyte cytosol. *Biomed. Res.* 16, 173–186.
- Twisk, J., Gillian-Daniel, D. L., Tebon, A., Wang, L., Barrett, P. H., and Attie, A. D. (2000). The role of the LDL receptor in apolipoprotein B secretion. *J. Clin. Investig.* 105, 521–532.
- Umlauf, E., Cszasz, E., Moertelmaier, M., Schuetz, G. J., Parton, R. G., and Prohaska, R. (2004). Association of stomatin with lipid bodies. *J. Biol. Chem.* 279, 23699–23709.
- Wakata, Y., Tokumoto, M., Horiguchi, R., Ishikawa, K., Nagahama, Y., and Tokumoto, T. (2004). Identification of alpha-type subunits of the *Xenopus* 20S proteasome and analysis of their changes during the meiotic cell cycle. *BMC Biochem.* 5, 18.
- Wiertz, E. J., Jones, T. R., Sun, L., Bogoy, M., Geuze, H. J., and Ploegh, H. L. (1996a). The human cytomegalovirus US11 gene product dislocates MHC class I heavy chains from the endoplasmic reticulum to the cytosol. *Cell* 84, 769–779.
- Wiertz, E. J., Tortorella, D., Bogoy, M., Yu, J., Mothes, W., Jones, T. R., Rapoport, T. A., and Ploegh, H. L. (1996b). Sec61-mediated transfer of a membrane protein from the endoplasmic reticulum to the proteasome for destruction. *Nature* 384, 432–438.
- Williams, K. J., Brocia, R. W., and Fisher, E. A. (1990). The unstirred water layer as a site of control of apolipoprotein B secretion. *J. Biol. Chem.* 265, 16741–16744.
- Wolins, N. E., Quaynor, B. K., Skinner, J. R., Schoenfish, M. J., Tzekov, A., and Bickel, P. E. (2005). S3-12, adipophilin, and TIP47 package lipid in adipocytes. *J. Biol. Chem.* 280, 19146–19155.